Disentangling the 1MLCT transition of [Ru(bpy)3]2+ by Stark absorption spectroscopy

doi: 10.1016/j.jphotochem.2017.08.025

Disentangling the ^{1}MLCT transition of $[Ru(bpy)_3]^{2+}$ by Stark absorption spectroscopy

Keisuke Kawamoto,[a] Yudai Tamiya,[b] Tim Storr,[c] Richard J. Cogdell,[d] Isamu Kinoshita,[b] Hideki Hashimoto[e,*]

[a] *Department of Chemistry, Graduate School of Science and Technology, Kanazawa University, Kakuma, Kanazawa 920-1192, Japan.*

[b] *The Osaka City University Advanced Research Institute for Natural Science and Technology (OCARINA), 3-3-138 Sugimoto, Sumiyoshi-ku, Osaka 558-8585, Japan.*

[c] *Department of Chemistry, Simon Fraser University, Burnaby, BC, V5A-1S6, Canada.*

[d] *Glasgow Biomedical Research Centre, Institute of Molecular Cell and Systems Biology, University of Glasgow, 126 University Place, Glasgow G12 8TA, Scotland, UK.*

[e] *Department of Applied Chemistry for Environment, School of Science and Technology, Kwansei Gakuin University, 2-1 Gakuen, Sanda, Hyogo 669-1337, Japan.*

*Corresponding Author, E-mail address: hideki-hassy@kwansei.ac.jp

Abstract: The metal-to-ligand charge transfer (MLCT) transition of $[Ru(bpy)_3]^{2+}$ was investigated using Stark absorption spectroscopy, where bpy is the abbreviation of 2,2'-bipyridyl ligand. The magnitude and direction of the photoinduced intramolecular charge transfer were precisely determined for the ^{1}MLCT transition of $[Ru(bpy)_3]^{2+}$. The ^{1}MLCT absorption band of $[Ru(bpy)_3]^{2+}$, observed in the 18,000—30,000 cm^{-1} spectral region, is composed of several sub-bands that can be approximated with Gaussian profiles. In particular, three distinct major ^{1}MLCT bands of $[Ru(bpy)_3]^{2+}$ (g4, 21272 cm^{-1}; g5, 22026 cm^{-1}; g7, 23448 cm^{-1}) could be distinguished by the direction of the charge transfer of each transition. The experimentally determined directions of charge transfer showed good agreement with the theoretical prediction by Kober and Meyer. We also

re-examined the phosphorescence and the excitation spectra of $[Ru(bpy)_3]^{2+}$. The ^{1}MLCT excited states of the g5 and g7 bands almost completely transform to ^{3}MLCT excited states, and then 40% of the ^{3}MLCT state relaxes to the ground state by emitting phosphorescence. 46% of ^{1}MLCT excited state of the g4 band non-radiatively relaxes to the ground state. These results provide good support for the assignment of the different origins of the g4 and other two Gaussian sub-bands (g5 and g7).

Keywords: Tris(2,2'-bipyridyl)ruthenium(II), metal-to-ligand charge transfer, change in dipole moment upon photoescitation (**Δμ**), charge-transfer direction, Stark absorption spectroscopy

1. Introduction

Using solar energy to generate clean, renewable electricity is becoming increasingly important in the drive to minimize the use of fossil fuels. In the conventional solar cell, the photoelectric conversion is achieved using a *p*-*n* junction of the semi-conductor devices [1]. On the other hand, dye-sensitized solar cells (DSSCs), which were originally invented and subsequently improved by Grätzel, utilize charge-separation induced by the internal electron transfer from sensitizer dye molecules [2]. Even though many different dyes have been tested, ruthenium (Ru) complexes are widely still being investigated as a dye molecule due to the excellent properties and stabilities [3]. This is because when Ru complexes are illuminated metal-to-ligand charge transfer (MLCT) transition states are generated that can readily go on to form Ru oxidation states up to +3, which can be injected into semiconductors. As an advantageous feature of a combination of a Ru complex as a photosensitizer and TiO_2 as a semiconductor, the electron injection process for DSSCs performance is unusually fast (as fast as 20 fs) [4, 5] in terms of Marcus theory [6]. The key roles of these MLCT states of $[Ru(bpy)_3]^{2+}$ (Figure 1) have, therefore, attracted significant attention over the past two decades in order to understand their exact photochemical properties [7].

However, in spite of the importance of these MLCT states in the generation of charge

separation in DSSCs, quantitative discussions of these states have been restricted to a few examples [8−15]. Stark absorption spectroscopy, for example, was applied by Boxer and coworkers as one of the methods for the determination of the change in dipole moment, $\mathbf{\Delta\mu}$, of the charge transfer in transition metal complexes [8]. These authors discussed the magnitude of $\mathbf{\Delta\mu}$ and the distance of the charge transfer from the Ru center to the bpy ligand. In contrast, there have been a significant number of theoretical studies. As reported by Kobar, three major MLCT transition bands of $[Ru(bpy)_3]^{2+}$ were theoretically assigned to ^1E (e (dπ) → e (π*)), ^1E (a_1 (dπ) → e (π*)), and ^1E (e (dπ) → a_2 (π*)) [9, 10]. The transition dipole moment of ^1E (e (dπ) → e (π*)) is predominated by the second term, the transfer term, in eq. (18) (see Theory section), since the dπ and π* orbitals have the same symmetry. Therefore, the direction of the transition dipole moment of ^1E (e (dπ) → e (π*)) and that of the charge transfer are parallel to each other. On the other hand, ^1E (a_1 (dπ) → e (π*)) is a forbidden transition based on the molecular orbital symmetry. However, the magnitude of the transition dipole moment does not become zero because this transition can borrow intensity from the intra-ligand allowed transition, a_1 (π) → e (π*), which corresponds to the third term in eq. (18) (see Theory section). Similarly ^1E (e (dπ) → a_2 (π*)) can be regarded as the vacant inter-orbital transition (^1E (e (π*) → a_2 (π*))) that reflects the reverse donation of e (dπ) → e (π*), and its transition dipole moment is governed by the fourth term in eq. (18) (see Theory section). Therefore, the directions of the transition dipole moments of the ^1E (a_1 (dπ) → e (π*)) and ^1E (e (π*) → a_2 (π*)) transitions are different from that of the charge-transfer. The above theoretical assignment of the MLCT transitions of $[Ru(bpy)_3]^{2+}$ has often been referred to in order to interpret the experimental data. From these theoretical predictions, it is important to determine the directions of charge transfer experimentally in order to test the validity of the theoretical assignments. Boxer and coworkers already determined the magnitude of $\mathbf{\Delta\mu}$ by using Stark absorption spectroscopy. However, they did not precisely discuss the charge-transfer direction, although this particular method can also be applicable to determine the direction of the charge transfer transition. In this present study, the directions of the MLCT transitions of $[Ru(bpy)_3]^{2+}$ have been determined by Stark absorption spectroscopy in addition to the

reinvestigation of the magnitude of **Δμ**, and in doing this, the validity of the theoretical MO model reported by Kobar has been experimentally addressed for the first time.

2. Materials and methods

2.1 Synthesis of a Ru complex

Tris(2,2'-bipyridyl)ruthenium(II) chloride hexahydrate, $[Ru(bpy)_3]Cl_2 \cdot 6H_2O$ was prepared as described in the literature [16]. The purity of the complex was confirmed from the UV-vis absorption spectrum in water and by ^1H NMR spectrum in D_2O.

2.2 Preparation of sample cells for Stark absorption measurements

Aqueous solutions of polyvinyl alcohol (PVA) polymer and $[Ru(bpy)_3]Cl_2 \cdot 6H_2O$ were prepared by the following method, respectively. PVA polymer (200 mg, PVA-217, Kuraray Co., Ltd) was dissolved in 2.0 mL of distilled water. The concentration of the solution of the Ru complex was set at an optical density of ca. 30 at its absorption maximum. The polymer and the complex solutions were then mixed in 50:50 (v/v) ratio. The sample cells for Stark absorption measurements were prepared by dropping this mixture on top of an interdigitated array of electrodes, separated by 50 μm gaps, which were made by vacuum deposition of aluminum on a cleaned glass substrate.

2.3 UV-vis absorption and photoluminescence measurements

Steady-state UV-vis absorption spectra were recorded on JASCO V-570 spectrophotometer at room temperature. Steady-state photoluminescence and photoluminescence excitation spectra were recorded on JASCO FP-6600 spectrofluorometer. The optical response of the fluorometer was calibrated using a standard lamp.

2.4 Stark absorption measurements

The details of the set-up for Stark absorption measurements have already been reported [17−20].

The electrodes on the Stark sample cell were connected with copper wires using electric conductive paste (Dotite). These copper wires were then connected to the output of a bipolar power amplifier (NF, 4305). A sinusoidal voltage of 500 Hz frequency was generated using a function generator (NF, E-1201A). The output voltage of the function generator was then amplified using the bipolar amplifier to 200 V. The light source used for Stark absorption measurements was a 150 W Xenon arc lamp (Hamamatsu, L2274) for the 325–625 nm wavelength range. The monochromatic light was obtained by dispersing the white light source using a monochromator (Acton Research, SpectraPro 150). The monochromatic light was then linearly polarized using a Glan-Thompson prism. The angle between the linear polarization of light and the electric field applied to the sample was controlled by rotating the Glan-Thompson prism. The light transmitted through the Stark cell was detected using a silicon photodiode (Hamamatsu, S1336-8BQ). The direct current (DC) component of the intensity of transmitted light was recorded by using a digital multi-meter (Fluke, 45), while that of the second harmonic of the alternating current (AC) component was selectively amplified using a dual phase lock-in amplifier (NF, 5610B). The Stark absorption spectra were calculated using these components according to the following mathematical formula.

$$\Delta A = -\log\frac{I_F - \Delta I}{I_F} \qquad (1),$$

where I_F is the intensity of the transmitted light without the application of the external electric field (the DC component), and ΔI is the change of the intensity of the transmitted light with the application of the external electric field (the AC component). All measurements were performed at 78 K using a liquid nitrogen cryostat (Oxford, Optistat DN).

3. Calculation

3.1 Analysis of Stark absorption spectra

The Stark absorption spectra were analyzed based on the theory developed by Liptay [21−25]. When a molecule is in isotropic environment, the Stark absorption spectrum can be described by the following equations.

$$\Delta A(\nu) = \left[A_\chi \cdot A(\nu) + B_\chi \cdot \frac{\nu}{15hc}\frac{d\left(A(\nu)/\nu\right)}{d\nu} + C_\chi \cdot \frac{\nu}{30h^2c^2}\frac{d^2\left(A(\nu)/\nu\right)}{d\nu^2}\right] \cdot |f \cdot \mathbf{E}|^2 \quad (2),$$

$$A_\chi = \frac{D}{3} + \frac{E}{30}(3\cos^2\chi - 1) \quad (3),$$

$$B_\chi = 5F + G(3\cos^2\chi - 1) \quad (4),$$

$$C_\chi = 5H + I(3\cos^2\chi - 1) \quad (5),$$

$$D = \frac{1}{|\mathbf{M}|^2}\sum_{ij}\left(X_{ii}X_{jj} + M_iY_{ijj}\right) \quad (6),$$

$$E = \frac{3}{|\mathbf{M}|^2}\sum_{ij}\left(X_{ij}^2 + X_{ij}X_{ji} + M_iY_{jij} + M_iY_{jji}\right) - 2D \quad (7),$$

$$F = \frac{1}{2}Tr(\mathbf{\Delta\alpha}) + \frac{2}{|\mathbf{M}|^2}\left(\sum_{ij} M_iX_{ij}\right) \cdot \mathbf{\Delta\mu} \quad (8),$$

$$G = \frac{3}{2}\mathbf{m} \cdot \mathbf{\Delta\alpha} \cdot \mathbf{m} - \frac{1}{2}Tr(\Delta\alpha) + \frac{3}{2}\frac{2}{|\mathbf{M}|^2}\left(\sum_{ij} M_iX_{ij}\right) \cdot \mathbf{\Delta\mu} \quad (9),$$

$$H = |\mathbf{\Delta\mu}|^2 \quad (10),$$

$$I = 3(\mathbf{m} \cdot \mathbf{\Delta\mu})^2 - |\mathbf{\Delta\mu}|^2 \quad (11).$$

Where ν is the frequency of the incident light, c is the speed of light in vacuum, h is the Planck's constant, f is the local-field correction factor, **E** is the externally applied field, **M** is the transition dipole moment, **m** is the unit vector for the transition dipole moment, **X** is the tensor of the transition dipole-moment polarizability, **Y** is the tensor of transition dipole-moment hyperpolarizability, **Δα** is the change in polarizability upon photoexcitation, and **Δμ** is the change in static dipole-moment upon photoexcitation. Vector and tensor components are denoted with boldface characters. Matrix components of the **M** vector, and **X** and **Y** tensors are denoted with subscripts of *i* and *j*, being equal to *x*, *y*, or *z* axis of a molecule. χ corresponds to the angle between linear polarization of incident

light and the direction of externally applied electric field. The coefficients A_χ, B_χ, and C_χ were obtained by the spectral fitting of the zero-th, first, and second derivative waveforms of the absorption spectrum to the observed Stark absorption spectra. When A_χ is negligible, B_χ and C_χ can be approximated as follows.

$$B_\chi \approx \frac{2}{5} Tr(\mathbf{\Delta\alpha}) + (3\cos^2\chi - 1)\left(\frac{3}{2}\mathbf{m}\cdot\mathbf{\Delta\alpha}\cdot\mathbf{m} - Tr(\mathbf{\Delta\alpha})\right) \quad (12),$$

$$C_\chi \approx 5|\mathbf{\Delta\mu}|^2 + (3\cos^2\chi - 1)(3(\mathbf{m}\cdot\mathbf{\Delta\mu})^2 - |\mathbf{\Delta\mu}|^2) \quad (13).$$

The values of Tr($\mathbf{\Delta\alpha}$) and $\left(\frac{3}{2}\mathbf{m}\cdot\mathbf{\Delta\alpha}\cdot\mathbf{m} - Tr(\mathbf{\Delta\alpha})\right)$ as well as $|\mathbf{\Delta\mu}|$ and $(3(\mathbf{m}\cdot\mathbf{\Delta\mu})^2 - |\mathbf{\Delta\mu}|^2)$ can be calculated by fitting eqs. (12) and (13) to the χ-angular dependence data of B_χ and C_χ. Consequently, the angle between $\mathbf{\Delta\alpha}$ and $\mathbf{m}$ as well as that between $\mathbf{\Delta\mu}$ and $\mathbf{m}$ can be determined using following equations.

$$\frac{\mathbf{m}\cdot\mathbf{\Delta\alpha}\cdot\mathbf{m}}{Tr(\mathbf{\Delta\alpha})} \approx \cos^2\theta_{\mathbf{\Delta\alpha}} \quad (14)$$

$$\frac{\mathbf{m}\cdot\mathbf{\Delta\mu}}{|\mathbf{\Delta\mu}|} = \cos\theta_{\mathbf{\Delta\mu}} \quad (15)$$

4. Theory

4.1 Transition dipole moment of MLCT described by the perturbation theory

In metal complexes exhibiting an MLCT absorption, the HOMO (φ_D) and LUMO (φ_A) states are regarded as being localized on the metal center and the ligand, respectively. However, these molecular orbitals can mix with various other molecular orbitals, as shown in eq. (16).

$$\begin{aligned}\phi_D &= \phi_d + \lambda_a\phi_{\pi^*} + \lambda_b\phi_\pi + \lambda_c\phi_{\pi'^*} \\ \phi_A &= \phi_{\pi^*} - \lambda_a\phi_d + \lambda_d\phi_p + \lambda_e\phi_{p^*}\end{aligned} \quad (16),$$

where *d*, *p* and *p** are, respectively, the *d*, *p* and unoccupied *p* orbitals of the metal center, and π and π^* are, respectively, the occupied and unoccupied π orbitals of the ligands, and π'^* is another unoccupied π orbital of the ligands that are not involved in MLCTs, and λ_a, λ_b, λ_c, λ_d, λ_e are coupling constants.

The transition dipole moment of a charge-transfer (CT) transition is defined as the integral

$$\mu_{CT} = -\int \psi_E er \psi_G d\tau = \langle \psi_E | \hat{\mu} | \psi_G \rangle \cong \langle \phi_A | \hat{\mu} | \phi_D \rangle \quad (17),$$

where $\hat{\mu}$ is the electric dipole moment operator. As shown in eq. (17), the transition dipole moment can be approximated as the integral of the molecular orbitals of the electron donor and the acceptor. Omitting terms of higher order, the transition dipole moment of the MLCT state, μ_{MLCT}, is represented by eq. (18), which can readily be derived from the substitution of eq. (16) into eq. (17),

$$\begin{aligned}\mu_{MLCT} = {} & \langle \phi_d | \hat{\mu} | \phi_{\pi^*} \rangle + \lambda_a \left(\langle \phi_{\pi^*} | \hat{\mu} | \phi_{\pi^*} \rangle - \langle \phi_d | \hat{\mu} | \phi_d \rangle \right) + \lambda_b \langle \phi_{\pi^*} | \hat{\mu} | \phi_\pi \rangle + \lambda_c \langle \phi_{\pi^*} | \hat{\mu} | \phi_{\pi'^*} \rangle \\ & + \lambda_d \langle \phi_p | \hat{\mu} | \phi_d \rangle + \lambda_e \langle \phi_{p^*} | \hat{\mu} | \phi_d \rangle \end{aligned} \quad (18),$$

where the first term is called the contact CT term and the second term the transfer term. Both of these terms represent a pure MLCT, while the transitions induced by the other terms are not pure MLCT. With regard to $[Ru(bpy)_3]^{2+}$, the contribution of the contact CT term to the MLCT transition can be ignored because the overlap of the molecular orbitals of the electron donor (ϕ_d) and acceptor (ϕ_{π^*}) is usually very small. On the other hand, the transfer term contains electron transfer from the *d* orbital of metal center to π^* orbital of the ligands, inducing the change in static dipole moment ($\mathbf{\Delta\mu}$) following the MLCT transition. Importantly, the direction of $\mathbf{\Delta\mu}$ should be parallel to that of transition dipole moment in the transfer term.

When the symmetries of the *d* and π^* orbitals are different, the coupling constant λ_a becomes zero. Then as a consequence the transfer term does not contribute at all to the MLCT transition. The transition dipole moment is due to the contact CT and the third to sixth terms in eq. (18). It should be noted that, in this case, the direction of the transition dipole moment induced by these terms is different from that of the charge-transfer.

5. Results and Discussion

The UV-vis absorption spectrum in the spectral region of the MLCT transition of $[Ru(bpy)_3]Cl_2 \cdot 6H_2O$ is shown in Figure 2. The broad spectral feature is successfully reproduced by the deconvolution using 10 Gaussian profiles. The result of this spectral deconvolution is also shown in Figure 2. The peak energies and full-width at half maxima (FWHM) of these Gaussian profiles are summarized in Table 1. Although the absorption spectrum in the 16000–28000 cm^{-1} regime can be well fitted using 10 Gaussian profiles, we focused our attention on the bands denoted as g4, g5, and g7 as these three MLCT sub-bands have already been well discussed based on the theoretical calculation by Kobar [9].

The composite material of a Ru complex and TiO_2 for DSSCs performs a very fast (as fast as 20 fs) [4, 5] charge injection from the Ru complex to the conduction band of TiO_2, which cannot be explained by Marcus theory [6]. We postulate that this very fast charge injection could occur directly from the Franc-Condon state of the ^{1}MLCT transition. In this study, Stark spectroscopy was measured to demonstrate the validity of the assignment for MLCT bands denoted as g4, g5, and g7. Although Boxer's report for the Stark spectroscopy of $[Ru(bpy)_3]^{2+}$ only described the magnitude of the charge transfer distances [8], we explore both the direction of the charge transfer as well as the reinvestigation of the magnitude of charge transfer distances. The Stark absorption spectra using three different polarization angles ($\chi = 0^o$, 54.7^o, and 90^o) are shown in Figure 3. The Stark spectra signals were observed only in the region of the g4 to g7 absorption bands, as only these bands have charge transfer character. Moreover, this experiment revealed that the charge transfer transitions are directed to only one bpy unit from the Ru center. Regarding the C_χ value in the Liptay equation, the dependence of the C_χ value on the polarization angles can be estimated in our technique (Figure 4). In addition, the angles between $\mathbf{\Delta\mu}$ and the transition dipole moment, **m**, were calculated by the fitting of these C_χ values (Table 2).

The assignment of the MLCT band for $[Ru(bpy)_3]^{2+}$ has usually been considered by theoretical analysis such as in Kobar's MO model. Using these theoretical arguments, the bands of g4, g5, and

g7 are assigned as follows. The g4 band can be assigned to a pure MLCT band, and it is predominated by the transfer term in Eq. (18) (^1E (e (dπ) → e (π*)). As already shown in the introduction section, in the MLCT absorption that is contributed mainly by the transfer term, the directions of the transition dipole moment of ^1E (e (dπ) → e (π*)) and that of the charge transfer are parallel to each other. The **Δμ** values (Table 2) represent the exited-state dipole moment because the D_3 point group molecule does not have a permanent dipole moment. Therefore, $\theta_{\Delta\mu}$ values (Table 2) correspond to the angles between the direction of the exited-state dipole moment and that of the transition dipole moment. The $\theta_{\Delta\mu}$ value of the g4 band is nearly zero (3.4°), and this experimental result clearly demonstrates the validity of the assignment of the origin of g4 band based on the theoretical analysis by Kobar. The absorption bands of g5 and g7 can be assigned to ^1E (a_1 (dπ) → e (π*)) and ^1E (e (dπ) → a_2 (π*)), respectively, and are dominated by the third and the fourth terms in Eq. (18). Therefore, the direction of the transition dipole moment of these absorptions is expected to be different from those of the charge-transfer. It is interesting to note that both the g5 and g7 bands have meaningful $\theta_{\Delta\mu}$ values (g5, 25.0°; g7, 21.2°). These experimental results again demonstrate the validity of the theoretical analysis by Kobar.

Furthermore, the magnitude of the charge transfer distances has been reinvestigated in this paper. The distances of the charge separation were calculated using **Δμ** values and elementary charges (Table 3). These distances and angles are compared to the X-ray structure, which was reported by Yufa et al. (CCDC 879418) [26]. The chemical structure of $[Ru(bpy)_3]^{2+}$ and the selected bond lengths and angles are summarized in Figure 5. The red dotted line in Figure 5 shows the direction of the transition dipole moment for the ^{1}MLCT transition at ca. 450 nm (22200 cm^{-1}). The direction of charge transfer of the g4 absorption band is from the Ru center to the central part of two pyridine units. On the other hand, those of g5 and g7 absorption bands are from the Ru center to the central part of the *meta* and *para* positions of a pyridine unit and to the *meta* position of a pyridine unit, respectively. As for the charge transfer distance from the Ru center to the bpy ligand, the g4 absorption band shows 40% of the distance between the Ru center and the central part of two

pyridine units. Those of g5 and g7 absorption bands are also about 30–40% of the distance between the Ru center and the central part of *meta* and *para* positions of a pyridine unit and *meta* position of a pyridine unit, respectively. In other words, the barycenter of charge deviates 30−40% from Ru center to the bpy ligand according to these ^{1}MLCT transitions.

We have also considered the ^{1}MLCT transition of the g4, g5, and g7 bands from the viewpoint of the photoluminescence and photoluminescence excitation spectra of $[Ru(bpy)_3]Cl_2 \cdot 6H_2O$ in H_2O. The photoluminescence of $[Ru(bpy)_3]Cl_2 \cdot 6H_2O$ in H_2O is observed at 16260 cm^{-1}, and it is assigned to the emission from a triplet excited state, *i.e.* this photoluminescence is ascribed to phosphorescence. The quantum yields of the intersystem crossing and the phosphorescence are >90% and ca. 40%, respectively [27]. In other words, some minor components are relaxed directly from ^{1}MLCT state to the ground state without showing intersystem crossing. For example, Chergui *et al.* have reported the femtosecond time-resolved fluorescence spectra of $[Ru(bpy)_3]^{2+}$, which is thought to be too fast as a radiative process [15]. The photoluminescence excitation spectrum of $[Ru(bpy)_3]Cl_2 \cdot 6H_2O$ in H_2O is shown in Figure 6, and comparison of the fractional absorbance (1 – Transmittance) and photoluminescence excitation spectra of $[Ru(bpy)_3]Cl_2 \cdot 6H_2O$ in H_2O show the coincidence of most of the peaks. However, spectral differences are evident in the region of g4 absorption band. This can be more easily recognized by taking the difference spectrum of the normalized fractional absorbance and photoluminescence excitation. A clear peak that corresponds to the g4 band is observed at 20964 cm^{-1}. This result can be interpreted as follows. 1) The ^{1}MLCT excited states of the g5 and g7 bands almost completely transform to ^{3}MLCT excited states, and then 40% of the ^{3}MLCT state relaxes to the ground state by emitting phosphorescence. 2) 46% of the ^{1}MLCT excited state of the g4 band non-radiatively relaxes to the ground state. Namely, the results of photoluminescence measurements also support the idea of the different origin of g4 and the other two bands (g5 and g7).

6. Conclusions

Although the transition dipole moment of the ^{1}MLCT for $[Ru(bpy)_3]^{2+}$ can be described as the sum of various components by perturbation theory, the predominant component is the transfer term. On the other hand, the contact CT term can be ignored, and the third and the fourth terms are not pure MLCT because these transitions occur by borrowing the intensity from the allowed intra-ligand transitions. As the ultrafast light-induced electron injection to a conduction band of a semiconductor occurs from a Franck-Condon active state of ^{1}MLCT [4, 5], the electron injection process might be dominated by the ^{1}MLCT state produced by the g4 absorption band. Therefore, to accelerate this electron injection process, a molecule must be designed so as to have a large enough oscillator strength on the transfer term's transition of the g4 band. Consequently, the directions of the charge transfer should be controlled depending on the proposed use of the chromophore molecules as sensitizers. The excitation energy dependence of the efficiency and rate of electron injection from ruthenium dye molecules to TiO_2 has been well determined [5]. The Stark spectroscopy performed in this present study is a useful tool to disentangle the origin of the MLCT transitions, and will be indispensable for obtaining deeper insight into the electron injection process and the structural basis of MLCT transitions.

Acknowledgements

HH thanks JSPS KAKENHI, Grant-in-Aids for Basic Research (B) (No. 16H04181) and Scientific Research on Innovative Areas "All Nippon Artificial Photosynthesis Project for Living Earth (AnApple)" (No. 24107002) for financial support. TS acknowledges a NSERC Discovery Grant. RJC wishes to gratefully thank the BBSRC and Photosynthetic Antenna Research Center (PARC), an Energy Frontier Research Center funded by the DOE, Office of Science, Office of Basic Energy Sciences under Award Number DE-SC 0001035 for financial support.

References

[1] A.F. Collings, C. Critchley, Artificial photosynthesis : from basic biology to industrial application, Wiley-VCH, 2005.

[2] B. O'Regan, M. Grätzel, A low-cost, high-efficiency solar cell based on dye-sensitized colloidal TiO_2 films, Nature 353 (1991) 737–740. doi:10.1038/353737a0.

[3] B. Pashaei, H. Shahroosvand, M. Graetzel, M.K. Nazeeruddin, Influence of Ancillary Ligands in Dye-Sensitized Solar Cells, Chem. Rev. 116 (2016) 9485–9564. doi:10.1021/acs.chemrev.5b00621.

[4] B. Wenger, M. Grätzel, J. E. Moser, Rationale for Kinetic Heterogeneity of Ultrafast Light-Induced Electron Transfer from Ru(II) Complex Sensitizers to Nanocrystalline TiO_2, J. Am. Chem. Soc. 127 (2005) 12150–12151. doi:10.1021/ja042141x.

[5] J.B. Asbury, N. a Anderson, E. Hao, X. Ai, T. Lian, Parameters Affecting Electron Injection Dynamics from Ruthenium Dyes to Titanium Dioxide Nanocrystalline Thin Film †, J. Phys. Chem. B. 107 (2003) 7376–7386. doi:10.1021/jp034148r.

[6] R.A. Marcus, Electron Transfer Reactions in Chemistry: Theory and Experiment (Nobel Lecture), Angew. Chem. Int. Ed. Engl. 32 (1993) 1111–1121. doi:10.1002/anie.199311113.

[7] D.W. Thompson, A. Ito, T.J. Meyer, $[Ru(bpy)_3]^{2+}$* and other remarkable metal-to-ligand charge transfer (MLCT) excited states, Pure Appl. Chem. 85 (2013) 1257–1305. doi:10.1351/PAC-CON-13-03-04.

[8] D.H. Oh, S.G. Boxer, Stark effect spectra of $Ru(diimine)_3^{2+}$ complexes, J. Am. Chem. Soc. 111 (1989) 1130–1131. doi:10.1021/ja00185a054.

[9] E.M. Kober, T.J. Meyer, Concerning the absorption spectra of the ions $M(bpy)_3^{2+}$ (M = Fe, Ru, Os; bpy = 2,2'-bipyridine), Inorg. Chem. 21 (1982) 3967–3977. doi:10.1021/ic00141a021.

[10] E.M. Kober, T.J. Meyer, An electronic structural model for the emitting MLCT excited states of $Ru(bpy)_3^{2+}$ and $Os(bpy)_3^{2+}$, Inorg. Chem. 23 (1984) 3877–3886. doi:10.1021/ic00192a009.

[11] F. Felix, J. Ferguson, H.U. Guedel, A. Ludi, The electronic spectrum of tris(2,2'-bipyridine)ruthenium(2+), J. Am. Chem. Soc. 102 (1980) 4096–4102. doi:10.1021/ja00532a019.

[12] A. Ceulemans, L.G. Vanquickenborne, Charge-transfer spectra of iron(II)- and ruthenium(II)-tris(2,2'-bipyridyl) complexes, J. Am. Chem. Soc. 103 (1981) 2238–2241. doi:10.1021/ja00399a017.

[13] B.J. Coe, J.A. Harris, B.S. Brunschwig, I. Asselberghs, K. Clays, J. Garín, J. Orduna, Three-Dimensional Nonlinear Optical Chromophores Based on Metal-to-Ligand Charge-Transfer from Ruthenium(II) or Iron(II) Centers, J. Am. Chem. Soc. 127 (2005) 13399–13410. doi:10.1021/ja053879x.

[14] N.H. Damrauer, G. Cerullo, A. Yeh, T.R. Boussie, C. V. Shank, J.K. McCusker, Femtosecond Dynamics of Excited-State Evolution in $[Ru(bpy)_3]^{2+}$, Science 275 (1997) 54–57. doi:10.1126/science.275.5296.54.

[15] A. Cannizzo, F. van Mourik, W. Gawelda, G. Zgrablic, C. Bressler, M. Chergui, Broadband Femtosecond Fluorescence Spectroscopy of $[Ru(bpy)_3]^{2+}$, Angew. Chem., Int. Ed. 45 (2006) 3174–3176. doi:10.1002/anie.200600125.

[16] J.A. Broomhead, C.G. Young, P. Hood, Inorganic Syntheses, John Wiley & Sons, Inc., Hoboken, NJ, USA, 1982. doi:10.1002/9780470132524.

[17] H. Hashimoto, T. Nakashima, K. Hattori, T. Yamada, T. Mizoguchi, Y. Koyama, T. Kobayashi, Structures and non-linear optical properties of polar carotenoid analogues, Pure Appl. Chem. 71 (1999) 2225–2236. doi:10.1351/pac199971122225.

[18] K. Yanagi, T. Kobayashi, H. Hashimoto, Origin of transition dipole-moment polarizability and hyperpolarizability in hydrazones, Phys. Rev. B. 67 (2003) 115–122. doi:10.1103/PhysRevB.67.115122.

[19] K. Yanagi, H. Hashimoto, A.T. Gardiner, R.J. Cogdell, Stark spectroscopy on the LH2 complex from Rhodobacter sphaeroides strain G1C; frequency and temperature dependence, J. Phys. Chem. B. 108 (2004) 10334–10339. doi:10.1021/jp037863+.

[20] T. Horibe, P. Qian, C.N. Hunter, H. Hashimoto, Stark absorption spectroscopy on the carotenoids bound to B800-820 and B800-850 type LH2 complexes from a purple photosynthetic bacterium, *Phaeospirillum molischianum* strain DSM120, Arch. Biochem. Biophys., 572 (2015) 158–166. doi: 10.1016/j.abb.2014.12.015.

[21] W. Liptay, Dipole Moments and Polarizabilities of Molecules in Excited Electronic States, in: Excited States, 1974: pp. 129–229. doi:10.1016/B978-0-12-227201-1.50009-7.

[22] W. Liptay, R. Wortmann, R. Böhm, N. Detzer, Excited state dipole moments and polarizabilities of centrosymmetric and dimeric molecules. II. Polyenes, polyynes and cumulenes, Chem. Phys. 120 (1988) 439–448. doi:10.1016/0301-0104(88)87230-6.

[23] D.H. Oh, S.G. Boxer, Electrochromism in the near-infrared absorption spectra of bridged ruthenium mixed-valence complexes, J. Am. Chem. Soc. 112 (1990) 8161–8162. doi:10.1021/ja00178a047.

[24] D.H. Oh, M. Sano, S.G. Boxer, Electroabsorption (Stark effect) spectroscopy of mono- and biruthenium charge-transfer complexes: measurements of changes in dipole moments and other electrooptic properties, J. Am. Chem. Soc. 113 (1991) 6880–6890. doi:10.1021/ja00018a026.

[25] G.U. Bublitz, S.G. Boxer, STARK SPECTROSCOPY: Applications in Chemistry, Biology, and Materials Science, Annu. Rev. Phys. Chem. 48 (1997) 213–242. doi:10.1146/annurev.physchem.48.1.213.

[26] K.S. Low, J.M. Cole, X. Zhou, N. Yufa, Rationalizing the molecular origins of Ru- and Fe-based dyes for dye-sensitized solar cells, Acta Crystallogr. Sect. B Struct. Sci. 68 (2012) 137–149. doi:10.1107/S0108768112009263.

[27] G.A. Crosby, J.N. Demas, Quantum efficiencies on transition metal complexes. II. Charge-transfer luminescence, J. Am. Chem. Soc. 93 (1971) 2841–2847. doi:10.1021/ja00741a003.

Figures

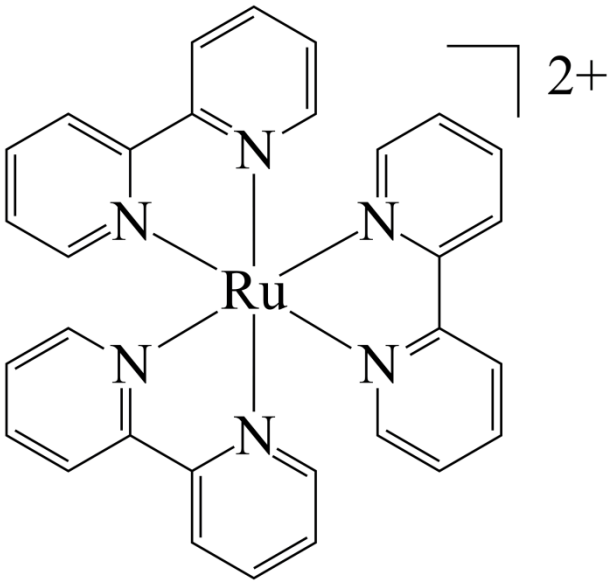

Figure 1. Chemical structure of $[Ru(bpy)_3]^{2+}$.

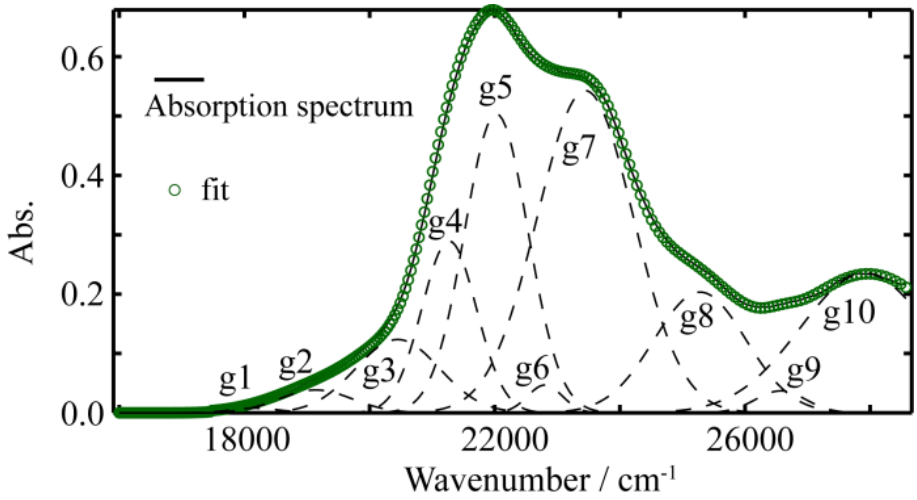

Figure 2. UV-vis absorption spectrum (–) of $[Ru(bpy)_3]Cl_2 \cdot 6H_2O$ in H_2O, and the results of the Gaussian curve-fitting (○). Each Gaussian component is drawn with dashed line.

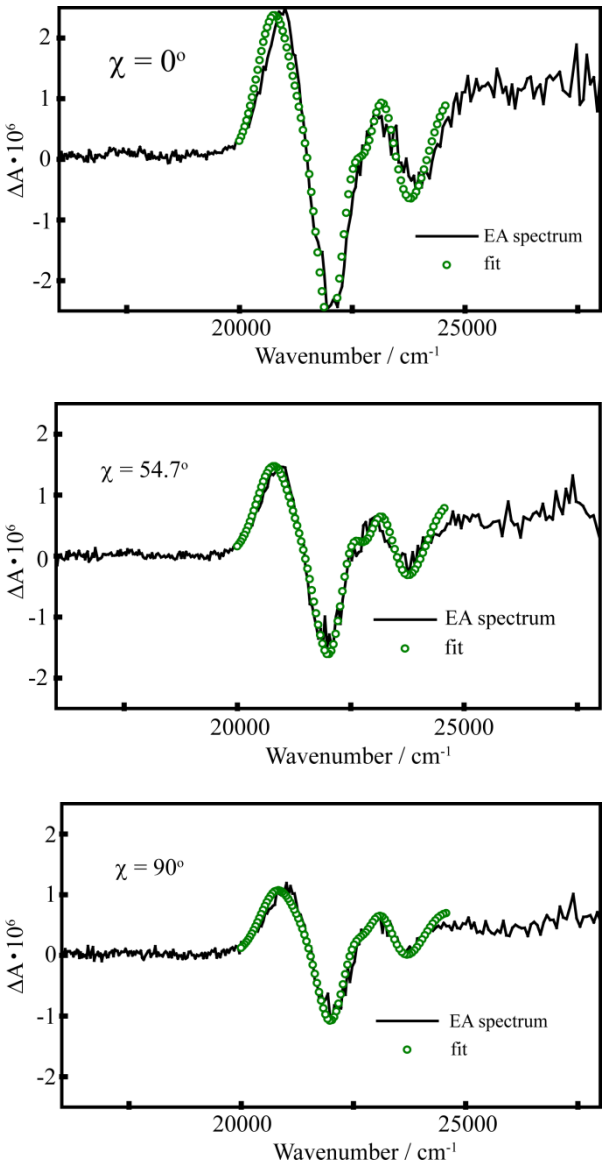

Figure 3. Stark absorption spectra (–) of the film of $[Ru(bpy)_3]Cl_2 \cdot 6H_2O$ in PVA recorded at $\chi = 0^o$, 54.7^o and 90^o. The results of spectral fittings are shown with green circles.

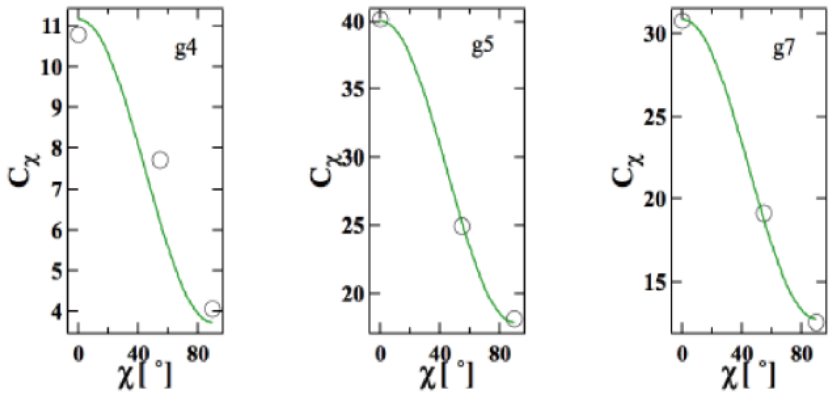

Figure 4. Angular dependence of C_χ values of the g4, g5, and g7 bands.

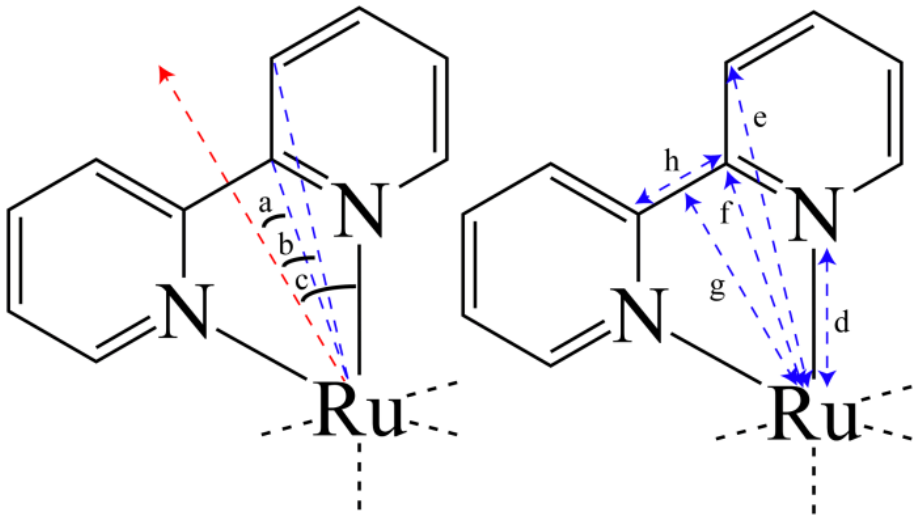

Figure 5. X-ray structural data overlaid on the partial chemical structure of $[Ru(bpy)_3]^{2+}$ [26]. Selected bond lengths (Å) and angles (^{o}) are as follows: a, 14^o; b, 21^o; c, 39^o; d, 2.07 Å ; e, 4.26 Å ; f, 2.92 Å; g, 2.82 Å ; h, 1.46 Å. The red dotted line shows the direction of transition dipole moment of ^{1}MLCT transition.

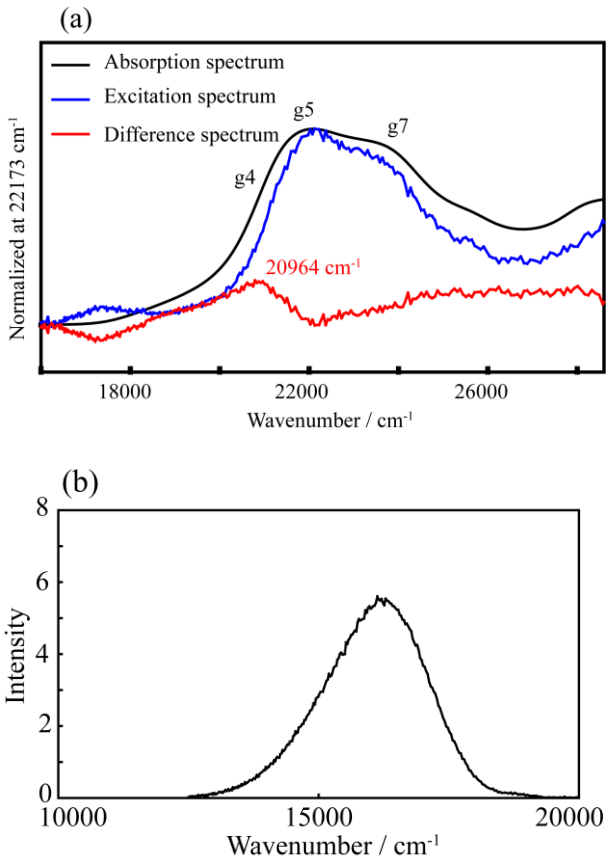

Figure 6. (a) Absorption spectrum (fractional absorbance, 1 – Transmittance), photoluminescence excitation spectrum recorded at 16260 cm^{-1} of $[Ru(bpy)_3]Cl_2 \cdot 6H_2O$ in water. The difference spectrum between fractional absorbance and photoluminescence excitation was obtained after normalization at 22173 cm^{-1}. (b) Emission spectrum of $[Ru(bpy)_3]Cl_2 \cdot 6H_2O$ in water at room temperature (λ_{ex}, 22222 cm^{-1}).

Tables

Table 1. The peak valuses (cm^{-1}, up) and the full width at half maximum (FWHM) (cm^{-1}, down) of Gaussian sub-bands obtained by the deconvolution of absorption spectrum of $[Ru(bpy)_3]Cl_2 \cdot 6H_2O$ in water

g1	g2	g3	g4	g5	g6	g7	g8	g9	g10
18174	19141	20448	21272	22026	22804	23448	25281	26570	27915
904	1414	1698	1060	1226	614	1904	1724	1108	2532

Table 2. The change in dipole moment (**Δμ**) and the angle between **Δμ** and **m** of g4, g5, and g7 bands

	g4	g5	g7
$\lvert \boldsymbol{\Delta\mu} \rvert$ (D/f)	3.34	6.74	5.81
$\theta_{\Delta\mu}$ (°)	3.4	25.0	21.2

Table 3. The **Δμ** values per electron and the distances of the charge separation induced by the transitions of g4, g5, and g7 bands

	g4	g5	g7
$\lvert \boldsymbol{\Delta\mu} \rvert$ ($C \cdot m/f \times 10^{-29}$)[a]	1.12	2.25	1.94
Distances of the charge separation (Å)[b]	0.70	1.40	1.21

[a] 1 debye, 3.34×10^{-30} C·m. [b] elementary electric charge, 1.602×10^{-19} C.